NEAR REAL-TIME MONITORING OF CASSAVA CULTIVATION AREA

Trong V. Phan [1, *)], Louis Reymondin [1)], Thibaud Vantalon [1)], Erik Delaquis [2)], Thuy T. Nguyen [1)] , Bandit Mienmany [2)]

1) International Center for Tropical Agriculture (CIAT), Vietnam country office. c/o Agricultural Genetics Institute, Pham Van Dong, Bac Tu Liem, Hanoi, Vietnam.
2) CIAT, Lao PDR country office. c/o NAFRI, Dong Dok, Ban Nongviengkham, PO box 783

* Corresponding author: t.v.phan@cgiar.org, Tel: +842437576969 / +84904443123

ABSTRACT: Remote sensing technologies and deep learning/machine learning approaches play valuable roles in crop inventory, yield estimation, cultivated area estimation, and crop status monitoring. Satellite-based remote sensing has led to increased spatial and temporal resolution, leading to a better quality of land-cover mapping (greater precision, and detail in the number of land cover classes). In this work, we propose to use a long short-term memory neural network (LSTM), an advanced technical model adapted from artificial neural networks (ANN) to estimate cassava cultivation area in southern Laos. LSTM is a modified version of a Recurrent Neural Network (RNN) that uses internal memory to store the information received prior to a given time. This property of LSTMs makes them advantageous for time series regression. We employ Landsat-7/8 and Sentinel-2 time-series datasets and crop phenology information to identify and classify cassava fields using multi-sources remote sensing time-series in a highly fragmented landscape. The results indicate an overall accuracy of > 89% for cassava and > 84% for all-class (barren, bush/grassland, cassava, coffee, forest, seasonal, and water) validating the feasibility of the proposed method. This study demonstrates the potential of LSTM approaches for crop classification using multi-temporal, multi-sources remote sensing time series.

Keywords: ***Cassava Mapping, Long Short-Term Memory (LSTM), Crop Classification, Deep Learning, Landsat-7/8, Remote Sensing, Sentinel-2, Multi-temporal, Google Earth Engine.***

1. INTRODUCTION

Cassava (*Manihot esculenta* Crantz) is a neotropical, Amazonian crop supplying one of the most important calorie sources in the global tropics and subtropics (Thiele et al., 2022). In the past several decades, Southeast Asian countries have adopted cassava as a major industrial crop linked to global export markets. In Lao PDR, the area of cassava cultivated is rapidly increasing, and in 2022 the root crop was the most valuable agricultural export, with 250 M USD exported in the first 6 months of the year (Lao Trade Portal, 2022). Cultivated primarily by smallholder farmers, cassava is a major contributor to rural incomes through the sale of fresh roots and dried chips to starch factories, commodity exporters, and intermediate traders forming the basis of cross-border value chains exporting to Thailand, Vietnam, and China (Delaquis et al., 2018). Nationally reported figures estimate 112,450 ha of cassava was planted in 2020, producing 3.5 M t of harvested roots (Lao Department of Agriculture, 2022). The rapid expansion of cassava cultivation in Laos has challenged authorities in accurately monitoring the rate at which fallow land, less profitable crops, and forested areas are converted to cassava plantations.

Many approaches exist to link vegetation index values and trends to a crop for specific cultivars (Johnson et al., 2014; Marshall et al., 2015; Reddy et al., 2018; Stepchenko et al., 2017). Current methodologies

based on remote sensing have been primarily developed and applied in high-value, large-scale, intensive agricultural systems such as maize, tomato, and grape in Peru (Tatsumi et al., 2015), maize and soybean in Canada (McNairn et al., 2014), barley and wheat in Ukraine (Kussul et al., 2015), and maize, soybean, wheat, and barley in Germany (RuBwurm et al., 2017). These approaches have been less commonly applied in developing countries, where agricultural landscapes are often highly fragmented with high heterogeneity of crop management and practices (Mishra et al., 2016). Current methodologies are poorly adapted to provide reliable crop area estimates at regional scales in the tropics. To address this gap, integrated remote sensing datasets processed with machine learning approaches are promising.

Deep learning is a powerful technique for processing remote sensing imagery (Han et al., 2012; Kamilaris et al., 2018; Zhang et al., 2016; Zhao et al., 2021). It has proved to be efficient for processing both optical (hyperspectral and multispectral) and radar images, and in extracting land cover types for crop mapping, road extraction, and building extraction applications (Chen et al., 2014; Geng et al., 2015; Kussul et al., 2017). Convolutional Neural Network (CNN) models have been employed in identifying crops (Long Short-Term Memory models (LSTM) + SVM) (Ienco et al., 2017), and crop types in time series (three-unit LSTM, CNN, SVM) (Rußwurm et al., 2018). Deep auto-encoders, deep belief networks, and recurrent neural networks with LSTM models are promising for remote sensing tasks (Kussul et al., 2017).

We employed a large dataset of satellite imagery from southern Laos over 15 months in 2019/2020, and estimated cassava area through an LSTM implementation in the Google Earth Engine (GEE) and a local infrastructure using TensorFlow (Google, 2022). We present a framework for pre-processing, preparation of training data, and accuracy assessment, and discuss challenges in implementing the method over large areas.

2. MATERIALS AND METHODS

We utilized Landsat 7/8 and Sentinel-2 A/B time series imagery with high revisit time (10 days at the equator with one satellite, and 5 days with two satellites under cloud-free conditions which result in 2-3 days at mid-latitudes for sentinel-2, 16 days for Landsat 7/8 sensors) (ESA, 2022). We extracted a collection of images acquired over fifteen months to produce monthly mosaics over a study area located in Champassak and Attapeu provinces of Laos. Based on these mosaics, a training dataset was produced for mapping cassava areas considering aspects such as the local variability of land use land cover classes and potential spectral confusion. The monthly mosaics and training sets were used to build supervised classification models using LSTM algorithms. The resultant maps were evaluated with a stratified, randomly sampled validation dataset checked by three independent human interpreters against google earth and planet imagery. The datasets and methodological steps used in this study are presented in Figure 1 and are described in detail in the following sections.

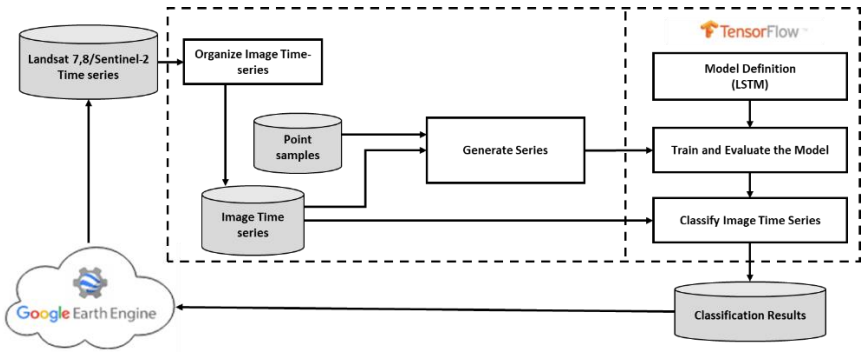

Figure 1: Schematic representation of data and methods used in the generation of cassava mapping in southern Laos.

2.1. Study area

The study area was in the adjacent southern Lao provinces of Champassak and Attapeu, bordering on Thailand to the west, Cambodia to the south, and Vietnam to the east (Figure 5). The area includes an altitudinal gradient rising from ~100m on the eastern banks of the Mekong River to ~1000m peaks of

the Bolaven plateau located from 15°28’54”-13°54’35”N, 105°28'0.23”-106°49’41”E. The agroecology of the region transitions from rice and vegetable dominated production in the river valleys to upland rice, coffee, rubber, and cassava plantations in the sloping uplands and plateau. While major agricultural areas of this region are accessible by road, it also includes remote forested conservation areas and sensitive subtropical semi-dry and moist forest ecosystems at risk of deforestation. This region also includes Laos’ 2nd most populous city, Pakse, and is one of the country’s fastest growing agricultural zones, including considerable increases in cassava exports in recent years.

2.2. Remotely sensed data

Images were obtained from Landsat-7/8 satellites (L7, L8) (OLI sensor), which has the United States Geological Service (USGS) as the official image provider, and Sentinel 2A and 2B satellites (S2) (MSI sensor) that are administered by the European Space Agency (ESA) (ESA, 2022). Recognizing that cassava is a long season crop with a typical 9-12 month cropping cycle, the periods chosen were from 01/10/2019 to 31/12/2020 to overlap with a full typical planting, growing, and harvesting cycle. After filtering images by period, we selected only images intersecting with the area of interest and with less than 90% cloud coverage according to their metadata.

The workflow for processing included three steps: 1) preprocessing, 2) sensor harmonization, and 3) post-processing. For pre-processing and sensor harmonization, we followed Nguyen et al. (2020) implementation of Poortinga et al. (2019). All images were obtained and pre-processed directly in GEE. In the preprocessing step, the clouds and their shadows are removed. The Bidirectional Reflectance Distribution Functions (BRDF) model was applied to reduce directional effects due to the differences in solar and view angles between L7/L8, and S2 and topographic correction was applied (Poortinga et al., 2019). The harmonization step included re-projection, re-scaling, and re-alignment (co-registration) of the L7, L8, and S2 images. After the processing, the images suffer from missing values due to the cloud removal algorithm. To fill the gaps, we applied a temporal interpolation algorithm on the GEE platform (Ujaval, 2021) to replace missing pixels with an interpolated value from its temporal neighbors. The leftover no-data gaps were filled by a temporal linear interpolation (Do Bendini et al., 2016), and the Savitzky–Golay smooth filter algorithm was used to smooth the data series fed into the model (Chen et al., 2021) to improve the resulting classification map (Figure 3). The final image processing step was a temporal aggregation of the individual images into monthly compositions using the mean value of the pixels. Using a monthly interval reduces requirements for downloading, storing, and processing data compared to individual images. Fifteen products corresponding from October 2019 to December 2020 were generated with six spectral bands (BLUE, RED, GREEN, NIR, SWIR1, SWIR2) and Normalized Difference Vegetation Index (NDVI), and used for training and classifying the models.

2.3. Model training and testing datasets

GPS points collected in the field were supplemented with Google Earth Pro and Planet imagery plugin on QGIS to collect cassava and non-cassava labeled samples to build the training, validation, and test datasets. Using the monthly mosaics and prior knowledge of the region, image interpretation experts collected 2,000 points for the cassava class and each of barren land, bush, forest, coffee, rice/seasonal, and water, resulting in 14,000-time series, each associated with a single point with pixels of only one land use land cover class, well-distributed throughout the study area and covering, as much as possible, all the land use land cover class variability observed. These points were used for classifier training and validation. For training and analysis of the accuracy of the models, 80% of the points were used for training, 10% were used for validation of the LSTM model, and 10% for testing.

2.4. Long short-term memory models

The RNN architecture we used employs Long Short-Term Memory (LSTM), a specific recurrent neural network architecture designed to model temporal sequences and their long-range dependencies more accurately than conventional RNNs (Sak et al., 2014), an important feature when working with longer time series. Each LSTM unit is designed to ‘remember’ values over arbitrary time intervals (long or short), improving efficiency when depicting variable temporal patterns such as those frequently observed in crop growing cycles (Zhong et al., 2019).

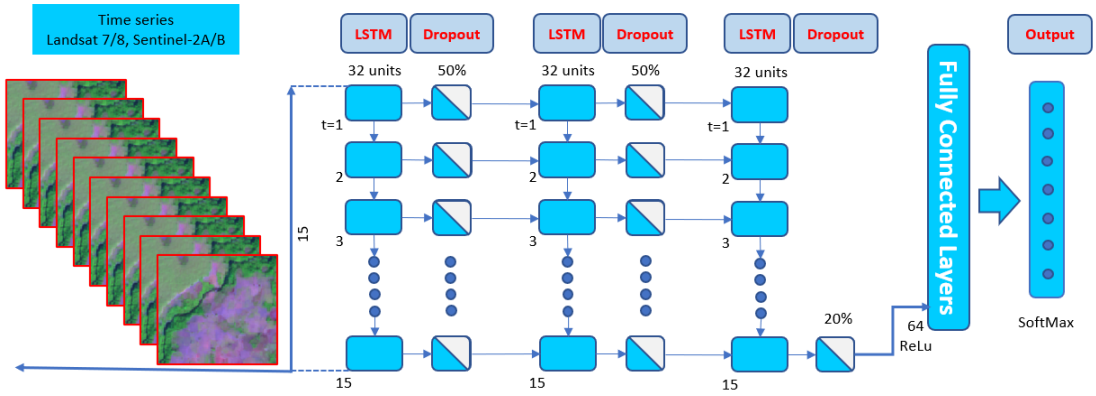

Figure 2: The structure of the optimal LSTM-based model employed for prediction of cassava area (adapted from Zhong et al., 2019).

The implementation of the LSTM classification approach (Zhong et al., 2019) is based on analyzing the spectral, spatial, and temporal dimensions of all monthly mosaics. To perform the classification task, we built a deep architecture stacking together three LSTM units (Figure 2). The use of multiple LSTM units, as commonly used for CNN networks combining several convolutional layers, allows for the extraction of high-level nonlinear temporal dependencies available in the remote sensing time series. This new representation is then fed to a dense neural network which assigns classes based on the new representation (Ienco et al., 2017). As a multiclass prediction, the output layer used the SoftMax activation function, while the other layers used the ReLu function (Parente et al., 2019). LSTM layers were used jointly with fully connected layers and dropout. We set the number of hidden dimensions equal to 32 units each. The probability of dropping neurons was set to 50%, 50%, and 20% for layers 1, 2, and 3, respectively, decreasing the chance of overfitting during model training (Parente et al., 2019). We set an initial learning rate of 0.001 and the last layer contained seven neurons corresponding to the probability of the seven classes. The neural network was trained for 100 epochs with a batch size equal to 16. We configured the model to use the Adam optimizer (Kingma et al., 2015), categorical cross-entropy loss function, and categorical accuracy as an evaluation metric, all parameters available in the TensorFlow library (Google, 2022). Finally, the trained model was used to classify all the pixels in the study area and produce a map showing the extent of cassava cultivation.

2.5. Land cover map validation protocol

Following Olofsson et al. (2014), validation was conducted on the binary map of cassava and non-cassava. We performed stratified random sampling to select 98 and 102 points in the cassava and non-cassava categories. Three human image interpreters independently reviewed each point using google imagery and assigned it a category. Points with disagreement amongst the interpreters were then reviewed and discussed as a group to assign a final category. In case of doubt or in case the google imagery was out-dated, the class was assigned based on the phenology observed on monthly Planet composite imagery obtained through the NICFI (Planet, 2022) program.

3. RESULTS AND DISCUSSION

3.1. Phenological curves of cassava

The intra annual NDVI curve of cassava has a well defined phenology corresponding with changes in the phenological stages of the crop growth cycle (Figure 3). In the study area cassava was planted from late May to early June and harvested during the period from late January to early February. This is reflected in the cassava NDVI spectral curves, which begin to increase from June until August, increase from mid-September to December, and decrease to bare soil during the harvest period.

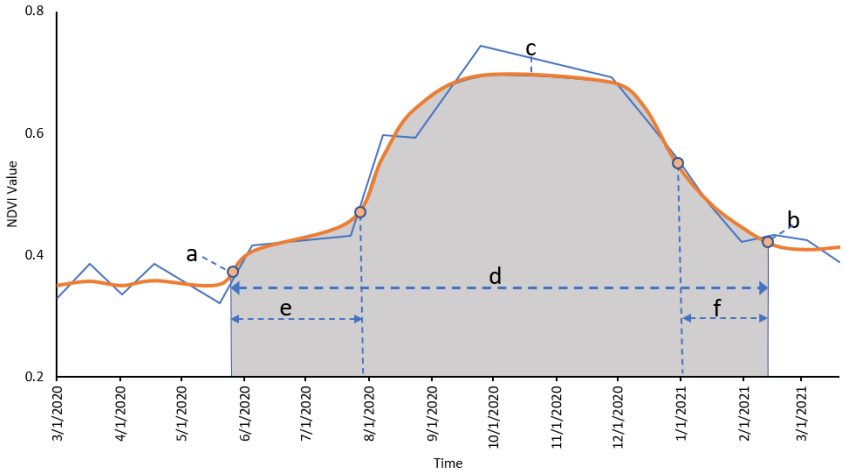

Figure 3: Examples of time-series NDVI spectral curves for cassava crop planted, (a) beginning of season, (b) end of season, (c) middle of season, (d) length of season, (e) time of planting, and (f) time of harvesting. The orange line represents the smoothed data, and the blue line is the original data.

3.2. Model calibration and accuracy assessment

LSTM classifiers were trained to classify time series versus other classes. In order to test model calibration, we computed the overall accuracy (OA), the kappa coefficient, the User, and Producer accuracies (UA and PA), and the F1 Score for each class based on the test set (10% of the training dataset not used for calibration). The LSTM accuracy metrics are illustrated in Figure 4. The overall accuracy was 93.43%, and the Kappa coefficient was 0.92. The results of the accuracy analysis using the validation dataset for the model developed for the UA, PA, and F1 provided by LSTM for cassava were 90%, 89%, and 89%, respectively. Evaluating the results, it is possible to verify that the model based on LSTM using the context of the entire time series for classification, achieved satisfactory accuracy to be used as input data for future analysis purposes.

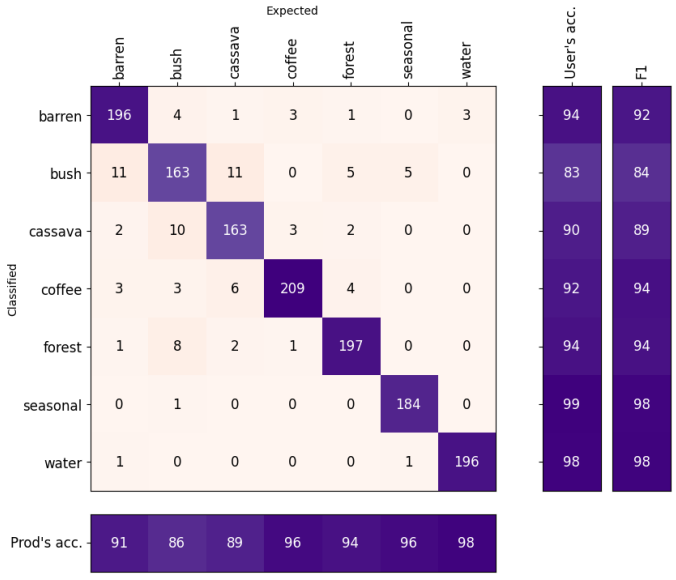

Figure 4: Accuracy analysis results with validation dataset from the model for the land use land classes observed in the study area.

3.3. Cassava Area Mapping

After evaluating the accuracy of the model, we used it to generate a map of land cover in the study area. Three subregions were selected randomly, and combined with high-resolution Google Satellite images in QGIS software to illustrate the output of the generated classification (Figure 5).

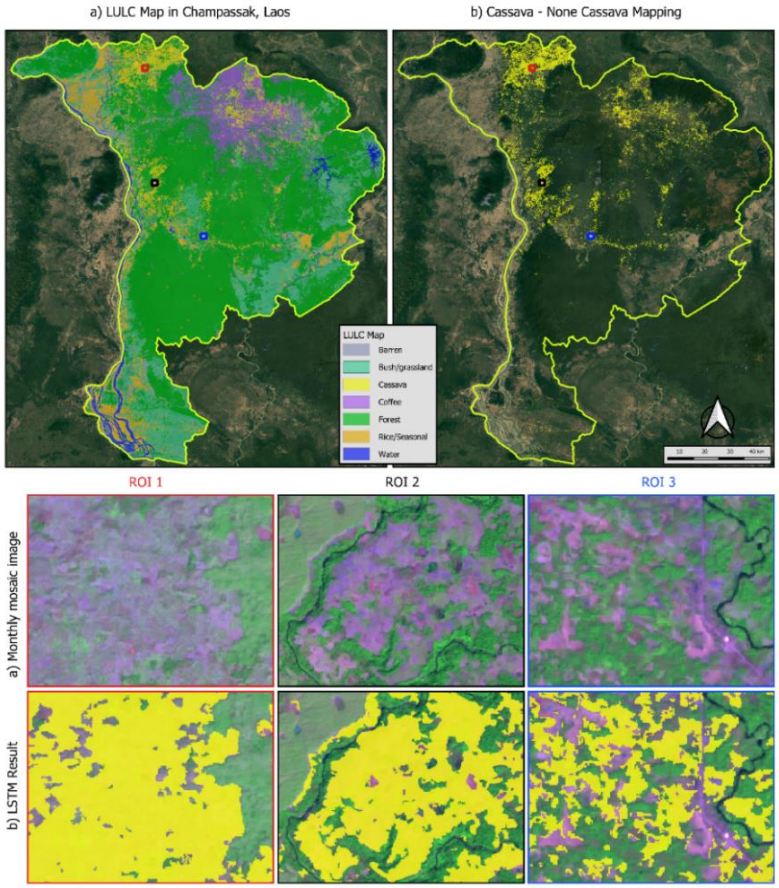

Figure 5: Land use land cover map in southern Laos: **a)** LULC map with seven classes and **b)** Cassava/Non-Cassava mapping and three subregions: **a)** monthly mosaic for November 2020 (RGB: SWIR1-NIR-RED bands) and **b)** the cassava maps produced with LSTM.

In the regions of interest (ROI 1 and ROI 2), LSTM better separated cassava areas, but in ROI 3 there was confusion between cassava with bush/grassland and other crops. Several pixels of cassava in the classified map were misclassified as tree crops, bush/grassland, and other crops, likely due to similarity between phenological curves of cassava and other classes in the rainfed study area (rice, corn, and scrubland). This misclassification was expected given the results of the model testing presented in Figure 4. For a better separation by LSTM, the number of training samples of cassava and other crops could be increased or sub-grouped.

Finally, the map produced through the LSTM model was validated based on a set of points randomly selected and visually validated by 3 independent interpreters. The results of the validation exercise, after normalization by area as proposed by Olofsson et al., (2014), show that the cassava/non-cassava map had an overall accuracy of 98% ± 2%. The cassava class had a UA of 83% ± 7% and PA of 83% ± 28%, while the non-cassava class had a UA and PA of 99% ± 2% and 99% ± 0% respectively. Cassava represented about 6% of the total studied area, while the non-cassava class encompassed the remaining 94%. The imbalance in the distribution of the classes lead to a high level of uncertainty in the estimation of the PA of the cassava class. As the UA of the cassava class is high and with low uncertainty, it might indicate that the cassava area shown in our results is a slight underestimation of the real extent.

4. CONCLUSIONS

The identification and mapping of cassava is a crucial step for land use management planning in Laos. This study demonstrates a methodology for generation of maps based on monthly data differentiating seven classes of land use and land cover within the study area. The application of several techniques for the compatibility and correction of satellite images allowed us to work with L7/8 and S2 images as a single collection to train machine learning models based on recurrent neural networks using the Long

short-term memory - LSTM neural network architecture. The LSTM-based model presented satisfactory results, with an average F1-Score of 89% for the cassava-mapped class.

The methods presented here can map large areas quickly, accurately, and inexpensively compared to traditional census-based approaches or expert manual interpretation of satellite images. The LSTM-based model presented superior results but requires retraining with additional samples to better model the variability of the land use classes in new regions. When applied to cassava-growing districts in Laos, this would allow for the validation of reported district production statistics, in addition to providing currently unavailable spatially explicit differentiation of expansion through cropland conversion or deforestation. An accurate and near-real time representation of changing cassava cropping patterns would enable decision makers to better monitor and regulate the cassava industry, forecast agricultural markets, and target agronomic or phytosanitary assistance initiatives. These abilities are critically important for building data-driven policy narratives and promoting sustainability and resilience in Laos' most valuable agricultural commodity.

5. REFERENCES

Chen, Y., Cao, R., Chen, J., Liu, L., & Matsushita, B., 2021. A practical approach to reconstruct high-quality Landsat NDVI time-series data by gap filling and the Savitzky–Golay filter. *ISPRS Journal of Photogrammetry and Remote Sensing*, 180, 174–190.

Chen, Y., Lin, Z., Zhao, X., Wang, G., & Gu, Y., 2014. Deep Learning-Based Classification of Hyperspectral Data. *IEEE Journal of Selected Topics in Applied Earth Observations and Remote Sensing*, 7(6), 2094–2107.

Delaquis, E., Andersen, K. F., Minato, N., Cu, T. T. le, Karssenberg, M. E., Sok, S., Wyckhuys, K. A. G., Newby, J. C., Burra, D. D., Srean, P., Phirun, I., Le, N. D., Pham, N. T., Garrett, K. A., Almekinders, C. J. M., Struik, P. C., & de Haan, S. (2018). Raising the Stakes: Cassava Seed Networks at Multiple Scales in Cambodia and Vietnam. *Frontiers in Sustainable Food Systems*, *2*, 73.

Do Bendini, H. N., Sanches, I. D., Körting, T. S., Fonseca, L. M. G., Luiz, A. J. B., & Formaggio, A. R., 2016. Using Landsat 8 image time series for crop mapping in a region of Cerrado, Brazil. *International Archives of the Photogrammetry, Remote Sensing and Spatial Information Sciences - ISPRS Archives*, *41*, 845–850.

ESA., 2022. Sentinel-2 - Missions - Sentinel Online - Sentinel Online. https://sentinel.esa.int/web/sentinel/missions/sentinel-2. Accessed: 15/09/2022.

Geng, J., Fan, J., Wang, H., Ma, X., Li, B., & Chen, F., 2015. High-Resolution SAR Image Classification via Deep Convolutional Autoencoders. *IEEE Geoscience and Remote Sensing Letters*, *12*(11), 2351–2355.

Google., 2022. *TensorFlow*. https://www.tensorflow.org/. Accessed: 15/09/2022.

Han, M., Zhu, X., & Yao, W., 2012. Remote sensing image classification based on neural network ensemble algorithm. *Neurocomputing*, *78*(1), 133–138.

Ienco, D., Gaetano, R., Dupaquier, C., & Maurel, P., 2017. Land Cover Classification via Multitemporal Spatial Data by Deep Recurrent Neural Networks. *IEEE Geoscience and Remote Sensing Letters*, *14*(10), 1685–1689.

Johnson, D. M., 2014. An assessment of pre- and within-season remotely sensed variables for forecasting corn and soybean yields in the United States. *Remote Sensing of Environment*, *141*, 116–128.

Kamilaris, A., & Prenafeta-Boldú, F. X., 2018. Deep learning in agriculture: A survey. *Computers and Electronics in Agriculture*, *147*, 70–90.

Kingma, D. P., & Lei Ba, J., 2015. Adam: A Method for Stochastic Optimization. *ICLR*.

Kussul, N., Lavreniuk, M., Skakun, S., & Shelestov, A., 2017. Deep Learning Classification of Land Cover and Crop Types Using Remote Sensing Data. *IEEE Geoscience and Remote Sensing Letters*, *14*(5), 778–782.

Kussul, N., Skakun, S., Shelestov, A., Lavreniuk, M., Yailymov, B., & Kussul, O., 2015. Regional scale crop mapping using multi-temporal satellite imagery. *ISPRS - International Archives of the Photogrammetry, Remote Sensing and Spatial Information Sci*ences, XL-7/W3, 45–52.

Lao Department of Agriculture., 2022. Annual Agricultural Yearbook 2020.

Lao Trade Portal., 2022. https://www.laotradeportal.gov.la/. Accessed: 15/09/2022.

Marshall, M., & Thenkabail, P., 2015. Developing in situ Non-Destructive Estimates of Crop Biomass to Address Issues of Scale in Remote Sensing. *Remote Sensing 2015, Vol. 7, Pages 808-835*, *7*(1), 808–835.

McNairn, H., Kross, A., Lapen, D., Caves, R., & Shang, J., 2014. Early season monitoring of corn and soybeans with TerraSAR-X and RADARSAT-2. *International Journal of Applied Earth Observation and Geoinformation*, *28*, 252–259.

Mishra, S., Mishra, D., & Santra, G. H., 2016. Applications of Machine Learning Techniques in Agricultural Crop Production: A Review Paper. *Indian Journal of Science and Technology*, *9*(38).

Nguyen, M. D., Baez-Villanueva, O. M., Bui, D. D., Nguyen, P. T., & Ribbe, L., 2020. Harmonization of Landsat and Sentinel 2 for Crop Monitoring in Drought Prone Areas: Case Studies of Ninh Thuan (Vietnam) and Bekaa (Lebanon). *Remote Sensing 2020, Vol. 12, Page 281*, *12*(2), 281.

Olofsson, P., Foody, G. M., Herold, M., Stehman, S. v., Woodcock, C. E., & Wulder, M. A., 2014. Good practices for estimating area and assessing accuracy of land change. *Remote Sensing of Environment*, *148*, 42–57.

Parente, L., Taquary, E., Silva, A. P., Souza, C., & Ferreira, L. (2019). Next Generation Mapping: Combining Deep Learning, Cloud Computing, and Big Remote Sensing Data. *Remote Sensing 2019, Vol. 11, Page 2881*, *11*(23), 2881.

Planet., 2022. NICFI Program - Satellite Imagery and Monitoring | Planet. https://www.planet.com/nicfi/. Accessed: 15/09/2022.

Poortinga, A., Tenneson, K., Shapiro, A., Nquyen, Q., Aung, K. S., Chishtie, F., & Saah, D., 2019. Mapping Plantations in Myanmar by Fusing Landsat-8, Sentinel-2 and Sentinel-1 Data along with Systematic Error Quantification. *Remote Sensing 2019, Vol. 11, Page 831*, *11*(7), 831.

Reddy, D. S., & Prasad, P. R. C., 2018. Prediction of vegetation dynamics using NDVI time series data and LSTM. *Modeling Earth Systems and Environment*, *4*(1), 409–419.

RuBwurm, M., & Korner, M., 2017. Temporal Vegetation Modelling Using Long Short-Term Memory Networks for Crop Identification from Medium-Resolution Multi-spectral Satellite Images. *2017 IEEE Conference on Computer Vision and Pattern Recognition Workshops (CVPRW)*, 1496–1504.

Rußwurm, M., & Körner, M., 2018. Multi-Temporal Land Cover Classification with Sequential Recurrent Encoders. *ISPRS International Journal of Geo-Information*, *7*(4), 129.

Sak, H., Senior, A., & Beaufays, F., 2014. Long Short-Term Memory Based Recurrent Neural Network Architectures for Large Vocabulary Speech Recognition.

Stepchenko, A., 2017. Land cover classification based on MODIS imagery data using artificial neural networks. *Vide. Tehnologija. Resursi - Environment, Technology, Resources*, *2*, 159–164.

Tatsumi, K., Yamashiki, Y., Canales Torres, M. A., & Taipe, C. L. R., 2015. Crop classification of upland fields using Random forest of time-series Landsat 7 ETM+ data. *Computers and Electronics in Agriculture*, *115*, 171–179.

Thiele, G., Friedmann, M., Campos, H. A., Polar, V., & Bentley, J. W., 2022. Root, tuber and banana food system innovations : value creation for inclusive outcomes. 561.

Ujaval., 2021. Temporal Gap-Filling with Linear Interpolation in GEE – *Spatial Thoughts*. https://spatialthoughts.com/2021/11/08/temporal-interpolation-gee/. Accessed: 15/09/2022.

Zhang, L., Zhang, L., & Du, B., 2016. Deep Learning for Remote Sensing Data: A Technical Tutorial on the State of the Art. *IEEE Geoscience and Remote Sensing Magazine*, *4*(2), 22–40.

Zhao, H., Duan, S., Liu, J., Sun, L., & Reymondin, L., 2021. Evaluation of Five Deep Learning Models for Crop Type Mapping Using Sentinel-2 Time Series Images with Missing Information. *Remote Sensing 2021, Vol. 13, Page 2790*, *13*(14), 2790.

Zhong, L., Hu, L., & Zhou, H., 2019. Deep learning based multi-temporal crop classification. *Remote Sensing of Environment*, *221*, 430–443.